

## Single photon emission from an InGaAs quantum dot precisely positioned on a nanoplane

Tung-Po Hsieh, Jen-Inn Chyi, Hsiang-Szu Chang, Wen-Yen Chen, Tzu Min Hsu, and Wen-Hao Chang

Citation: [Applied Physics Letters](#) **90**, 073105 (2007); doi: 10.1063/1.2644093

View online: <http://dx.doi.org/10.1063/1.2644093>

View Table of Contents: <http://scitation.aip.org/content/aip/journal/apl/90/7?ver=pdfcov>

Published by the [AIP Publishing](#)

---

### Articles you may be interested in

[Multiexcitonic emission from single elongated InGaAs/GaAs quantum dots](#)

J. Appl. Phys. **111**, 063522 (2012); 10.1063/1.3695458

[Single-photon emission from InGaAs quantum dots grown on \(111\) GaAs](#)

Appl. Phys. Lett. **96**, 093112 (2010); 10.1063/1.3337097

[Temperature stability of single-photon emission from InGaAs quantum dots in photonic crystal nanocavities](#)

Appl. Phys. Lett. **90**, 211114 (2007); 10.1063/1.2743398

[Optical emission from individual InGaAs quantum dots in single-defect photonic crystal nanocavity](#)

J. Appl. Phys. **98**, 034306 (2005); 10.1063/1.1953885

[Photon antibunching at high temperature from a single InGaAs/GaAs quantum dot](#)

Appl. Phys. Lett. **84**, 1260 (2004); 10.1063/1.1650032

---

The advertisement features a dark blue background with white and orange text. At the top left, it reads 'NEW! Asylum Research MFP-3D Infinity™ AFM' in large white letters, with 'Unmatched Performance, Versatility and Support' in orange below it. To the right is the Oxford Instruments logo, which includes the text 'OXFORD INSTRUMENTS' and 'The Business of Science®'. Below the main text are four images: a textured surface, a circular pattern, a grid of small squares, and the AFM instrument itself. Each image is accompanied by a short text description: 'Stunning high performance', 'Simpler than ever to GetStarted™', 'Comprehensive tools for nanomechanics', and 'Widest range of accessories for materials science and bioscience'.

# Single photon emission from an InGaAs quantum dot precisely positioned on a nanoplane

Tung-Po Hsieh and Jen-Inn Chyi<sup>a)</sup>

*Department of Electrical Engineering, National Central University, Zhongli 32001, Taiwan, Republic of China*

Hsiang-Szu Chang, Wen-Yen Chen, and Tzu Min Hsu

*Department of Physics, National Central University, Zhongli 32001, Taiwan, Republic of China*

Wen-Hao Chang

*Department of Electrophysics, National Chiao Tung University, Hsinchu 300, Taiwan, Republic of China*

(Received 19 November 2006; accepted 16 January 2007; published online 12 February 2007)

This work demonstrates single photon emissions from a site-controlled quantum dot (QD) grown on a self-constructed nanoplane. The size of the nanoplane on the micron-sized multifacet structure is accurately controlled by a low surface reducing rate ( $\sim 16$  nm/min). Single QD spectral lines were resolved and identified. The antibunching behavior reveals that single photons are emitted from the positioned QD. © 2007 American Institute of Physics. [DOI: 10.1063/1.2644093]

The single photon source is one of the most remarkable specialties of single quantum dots (QDs), which is unlike typically optical applications such as QD lasers and light emitting diodes. In recent years, single photon sources have been intensively investigated to develop quantum information processing, including quantum cryptography and quantum computing. Since advances in nanotechnology have improved the plasticity of semiconductor above that associated with single atoms or molecules, semiconductor QDs represent the main target of research into single photon sources.<sup>1,2</sup> Many researchers have studied single photons from single QDs. Self-assembled In(Ga)As QDs grown by molecular beam epitaxy<sup>1-3</sup> or metal organic chemical vapor deposition<sup>4,5</sup> (MOCVD) with high optical quality have until now been the main source of single QD. One of the main challenges to be overcome is to control the QD position since self-assembled QDs are randomly distributed. However, researchers are used to performing trial and error measurements on each indefinite QD to find a specific QD single photon source. Such an approach has slowed developments in physics and the decrease in the range of device applications. The spontaneous emission rate of single QDs was improved by exploiting the Purcell effect,<sup>6</sup> which governs the quantum electrodynamics in each cavity in the weak coupling region. Recently, highly efficient single photon sources have been produced by coupling single QDs into various microcavities, including microdisks,<sup>1</sup> microposts,<sup>7,8</sup> and photonic crystals.<sup>9,10</sup> However, the precise positioning of QDs in a particular position, which is required to control the coupling between QD emission and microcavity modes or produce single photon devices, remains difficult. Scientists must urgently develop the positioning of single QDs for single photon sources. Several researchers have attempted to find possible solutions to this problem, including surface indexing using vertically coupled QDs in a cavity QED system.<sup>11</sup> However, the use of many stack QDs has not exhibited single photon emissions. Self-assembled QDs grown on a prepatterned substrate exhibit great flexibility and potential in the

formation of a single QD system.<sup>12</sup> Another group has realized single photon emissions from the tip of a pyramidal structure on (311) GaAs substrate.<sup>5</sup> However, in the complex buffer layer removal process, (311) GaAs substrate and etched surface do not favor the development of single photon devices. This work demonstrates a deterministic approach for emitting single photons from a single spatially controlled QD grown on a self-constructed nanoplane. The size of a nanoplane on a multifaceted mesa can be controlled to limit the number of QDs.

The samples were grown by low-pressure MOCVD in a vertical reactor. Before QD growth, a GaAs substrate was patterned to form square mesa arrays (1–2  $\mu\text{m}$ ) by conventional photolithography. Then, a GaAs buffer layer was grown at 600 °C on the prepatterned substrate to reduce the top surface area while high-quality pyramidlike multifacet mesas with a top (100) nanoplane were self-formed. The resultant (100) surface decreased as the buffer layer grew, and its width was varied from 10 to 500 nm by controlling the mesa size and/or buffer layer growth time. Then, the substrate temperature was reduced to 500 °C to grow the QD layer. The indium content of the InGaAs QDs was set to 0.5 to ensure that the emission wavelength was within the detection range of the silicon detector. Self-assembled InGaAs QDs were selectively formed on the top (100) surface of the mesas. The number, distribution, and surface morphology of the QDs were determined using a scanning electron microscope (SEM). On some samples, an 80 nm thick GaAs cap layer was grown on top of the QDs for optical measurement. A closed-cycle cryostat combined with a high-resolution triple-grating spectrometer was established to make low-temperature ( $\sim 6$  K) microphotoluminescence ( $\mu\text{-PL}$ ) measurements. The single photon source was characterized using the Hanbury Brown and Twiss interferometer.

In this work, the size of the top (100) facet was controlled by adjusting the size of the original mesa and/or the thickness of the GaAs buffer layer. After the buffer layer was grown, the multifacets were formed as presented in Fig. 1(a). In the initial stage of GaAs buffer layer growth, the (100) surface was surrounded by two (111)*B* facets and four (124) facets, as shown in Fig. 1(b). As the thickness of the buffer

<sup>a)</sup>Electronic mail: chyj@ee.ncu.edu.tw

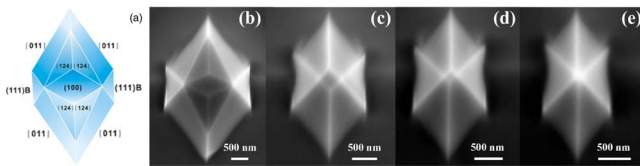


FIG. 1. (Color online) (a) Schematic multifaceted mesa with  $\{124\}$ ,  $\{110\}$ ,  $\{111\}$ , and  $\{100\}$  facets; [(b)–(e)] top-view SEM images of multifaceted mesas with  $\{100\}$  facet widths from 1300 to 20 nm.

layer increased, the  $\{110\}$  facets, rather than the  $\{124\}$  facets, dominated the multifaceted mesa, since the growth rate of the  $\{110\}$  facets is lower than that of the  $\{124\}$  facets.<sup>12</sup> As the mesa width declines from 1.5 to 1  $\mu\text{m}$ , the thickness of the  $\{100\}$  nanoplanes declines from 430 to 40 nm, as shown in Figs. 1(c)–1(e). Notably, the rate of decrease of the surface area is about 16 nm<sup>2</sup>/min, which is similar to the epitaxial growth rate, indicating that the number of QDs can be controlled by accurately tuning the top area size.

The authors recently demonstrated the growth of low-density QDs as single photon sources, by QD deposition under controlled growth conditions.<sup>5</sup> In this case, when ensemble low-density InGaAs QDs are grown on a multifaceted structure, they grew first on the edge of the  $\{100\}$  nanoplane because its surface energy is lower than that elsewhere, as shown in Fig. 2(a). On the top of the mesa, the adatoms diffused toward the edge of the nanoplane and left the center region free of QDs. As the thickness of QDs increases, more of the QDs form in the center of the mesa, while those at the mesa edge become large. In 1997, Kamins *et al.* reported the preferential location of Ge QDs on the top of the Si ridges with  $\{110\}$  sidewalls.<sup>13</sup> Similarly, InGaAs QDs also preferentially form along the edge of the narrow mesa with  $\{110\}$  and  $\{124\}$  sidewalls. According to the authors' previous experience,<sup>14</sup> a nanoridge with a width of 40–80 nm could grow reproducibly only as a single-line QD array. As the area of the top surface declines from 0.26 to 0.0054  $\mu\text{m}^2$ , the number of QDs falls to two or three, as shown in Figs. 2(b) and 2(c). When QDs were grown on a nanosurface with a width of  $48 \times 68 \text{ nm}^2$ , only a single QD was located on the top surface of the mesa, as shown in Fig. 2(d). Notably, no QD grows in the neighborhood of the rest of the facets of the structure since the critical thicknesses of the  $\{100\}$  top surface and  $\{110\}$  and  $\{124\}$  facets differ. In most reports, single photons are emitted by one of an ensemble low density QDs. Ensuring that other QDs are located near the desired QD is difficult before an optical measurement is made. In this case, a large area, at least 1  $\mu\text{m}^2$  depending on the structure size, is free of QDs. A two-level system that is purer than the aforementioned QD system can be constructed. For clarity, a two-dimensional  $\mu\text{-PL}$  mapping technique was adopted to determine whether only a QD is present on the multifaceted structure (not shown here). Fig-

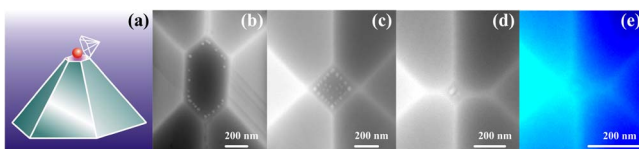


FIG. 2. (Color online) (a) Schematics of single QD grown on a multifaceted mesa; [(b)–(e)] top-view SEM images of single QDs grown on multifaceted mesas with various  $\{100\}$  surface areas.

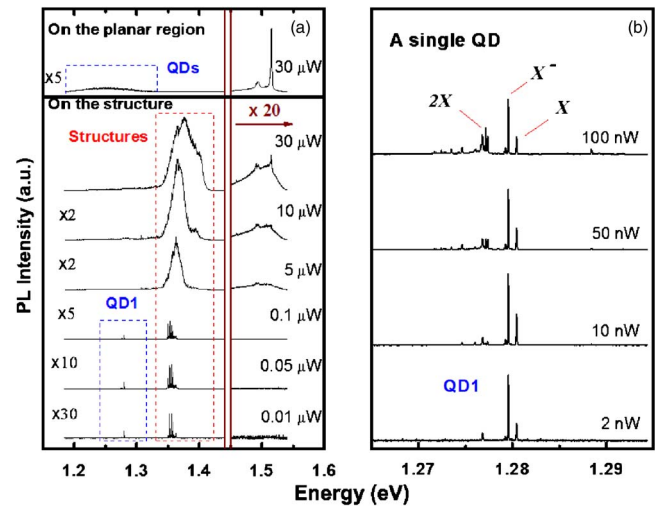


FIG. 3. (Color online)  $\mu\text{-PL}$  spectra of single QD on a multifaceted mesa at various excitation powers.

ure 2(e) schematically depicts a single QD grown on the multifaceted mesa as a single photon source.

Figure 3(a) presents the  $\mu\text{-PL}$  spectra of QDs in a planar region and on the multifaceted structure. The two spectra exhibit two similar peaks at 1.514 and 1.494 eV, corresponding to the GaAs band edge and the carbon impurity, respectively. Quantum dots in the planar region exhibit typical QD emission from 1.18 to 1.32 eV, while no clear wetting layer emission is observed. Figure 3(a) presents power-dependent  $\mu\text{-PL}$  spectra of the only QD located on the structure. The multifaceted structure yields an additional emission from 1.32 to 1.42 eV in addition to that from the QDs in the planar region. The additional emission is attributed to related quantum wires and/or wetting layers. The emission energy of the single QD is within the spectrum range of ensemble QDs in the planar region. A single QD emission and a few localized states of the structure dominate the emission process, yielding clear single QD peaks at low excitation powers.

The emission solid angle of a single QD in a planar structure is estimated to be about  $34^\circ$  due to total internal reflection, which leads to a low extraction efficiency ( $<10\%$ ). In our case, the extraction efficiency of single QDs embedded in this pyramidlike structure is expected to be doubled or even higher, because the emission solid angle is increased by the facets of pyramidal structure near the QD. In fact, the PL emission from single QDs on the structure is only stronger than that from those on the planar region by about 1.3 times. The difference between the experimental and expected values could be ascribed to the variation of optical properties across the sample. Figure 3(b) presents the low-power-dependent  $\mu\text{-PL}$  spectra of the single QD. The two emission peaks at 1.2771 and 1.2805 eV originate from the biexciton state ( $2X$ ) and the exciton state ( $X$ ), respectively, as revealed by the linear and quadratic dependences of PL intensity on power, as presented in Fig. 4(a). Another strong peak at 1.2796 eV with a linewidth of 65  $\mu\text{eV}$  exhibits similar power dependence to that of the exciton line. This line is assigned to the negatively charged exciton state ( $X^-$ ). The formation of charged excitons is typically related to impurities near the QD. In samples grown by MOCVD, and especially in the layer grown at low temperature ( $\sim 500^\circ\text{C}$ ), the unintentionally doped carbon impurities are



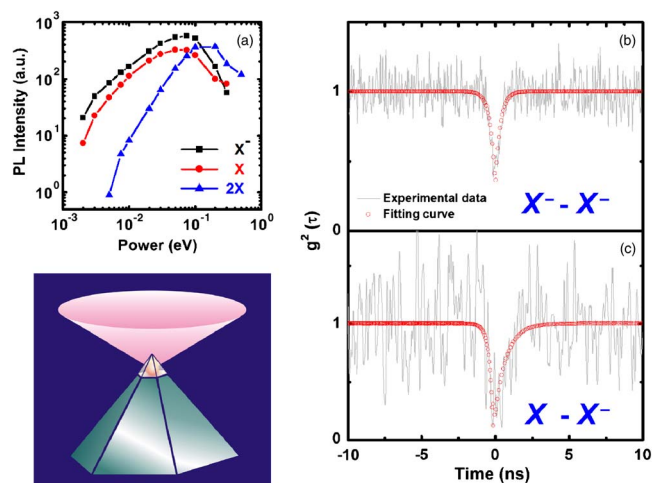


FIG. 4. (Color online) (a) Integrated PL intensities of the  $X$ ,  $X^-$ , and  $2X$  lines at various excitation powers; (b) autocorrelation function of the  $X^-$  line of the QD; and (c) cross-correlation function between the  $X^-$  and  $X$  lines.

important. Optically controlling the  $X$  and  $X^-$  lines using the carbon impurities has been discussed elsewhere.<sup>15</sup>

In a further analysis of QD emissions, autocorrelation measurements on the  $X^-$  line of the QD are made. Clear photon antibunching behavior, with a normalized depth of  $g^2(\tau)=0.36$ , reveals single photon emission from the QD, as presented in Fig. 4(b). Time-resolved PL measurements indicate that the radiative lifetime of the exciton is 0.84 ns, which is similar to that of  $X^-$  from QDs on a planar surface. The nonzero coincidence is caused primarily by the finite time resolution of our Hanbury Brown and Twiss setup and the background emission in the spectral measurements. The relationship between the  $X$  and  $X^-$  lines was elucidated by making cross-correlation measurements, as shown in Fig. 4(c). The starting and stopping signals are provided by the  $X$  and  $X^-$  lines, respectively. An asymmetric antibunching dip reveals that both lines originated from the same QD, but were associated with different QD excitonic species. The longer recovery time for  $\tau > 0$  in the cross correlation confirms that  $X^-$  is a negatively charged exciton state, because of the relatively shorter (longer) time scale required for recapturing one hole (two electrons and one hole) to form an  $X$  ( $X^-$ ) state after the emission of an  $X^-$  ( $X$ ) photon.<sup>15,16</sup> The spectral lines associated with the exciton, biexciton and

charged exciton were resolved and identified.

In summary, a single QD was grown on the nanoplane of a multifaceted structure. The size of the nanoplane was well controlled using a low surface reducing rate ( $\sim 16$  nm/min). Single photon emissions are verified by the antibunching behavior of the charged exciton line determined by making autocorrelation measurements. The efficiency of single photons is a little high due to the high extraction efficiency. This work represents a large step toward the deterministic spatial control of QD for highly efficient and highly pure single photon sources. It also provides the possibility of forming lateral and/or vertical coupled QDs for future quantum dot molecules and quantum bits.

This work was partially supported by the National Science Council of R.O.C. under Contract Nos. 94-2215-E-008-004 and 94-2752-E-008-001-PAE and the Center for Nano Science and Technology of the University System of Taiwan.

<sup>1</sup>P. Michler, A. Kiraz, C. Becher, W. V. Schoenfeld, P. M. Petroff, L. Zhang, E. Hu, and A. Imamoglu, *Science* **290**, 2282 (2000).

<sup>2</sup>C. Santori, M. Pelton, G. Solomon, Y. Dale, and Y. Yamamoto, *Phys. Rev. Lett.* **86**, 1502 (2001).

<sup>3</sup>Z. Yuan, B. E. Kardynal, R. M. Stevenson, A. J. Shields, C. J. Lobo, K. Cooper, N. S. Beattie, D. A. Ritchie, and M. Pepper, *Science* **295**, 102 (2002).

<sup>4</sup>M. H. Baier, E. Pelucchi, E. Kapon, S. Varoutsis, M. Gallart, I. Robert-Philip, and I. Abram, *Appl. Phys. Lett.* **84**, 648 (2004).

<sup>5</sup>T.-P. Hsieh, H.-S. Chang, W.-Y. Chen, W.-H. Chang, T. M. Hsu, N.-T. Yeh, W.-J. Ho, P.-C. Chiu, and J.-I. Chyi, *Nanotechnology* **17**, 512 (2006).

<sup>6</sup>E. M. Purcell, *Phys. Rev.* **69**, 681 (1946).

<sup>7</sup>E. Moreau, I. Robert, J. M. Gérard, I. Abram, L. Manin, and V. Thierry-Mieg, *Appl. Phys. Lett.* **79**, 2865 (2001).

<sup>8</sup>M. Pelton, C. Santori, J. Vuckovic, B. Zhang, G. S. Solomon, J. Plant, and Y. Yamamoto, *Appl. Phys. Lett.* **86**, 3903 (2001).

<sup>9</sup>D. Englund, D. Fattal, E. Waks, G. Solomon, B. Zhang, T. Nakaoka, Y. Arakawa, Y. Yamamoto, and J. Vuckovic, *Phys. Rev. Lett.* **95**, 013904 (2005).

<sup>10</sup>W.-H. Chang, W.-Y. Chen, H.-S. Chang, T.-P. Hsieh, J.-I. Chyi, and T.-M. Hsu, *Phys. Rev. Lett.* **96**, 117401 (2006).

<sup>11</sup>A. Badolato, K. Hennessy, M. Atature, J. Dreiser, E. Hu, P. M. Petroff, and A. Imamoglu, *Science* **308**, 1158 (2005).

<sup>12</sup>C.-K. Hahn, J. Motohisa, and T. Fukui, *Appl. Phys. Lett.* **76**, 3947 (2000).

<sup>13</sup>T. I. Kamins and R. S. Williams, *Appl. Phys. Lett.* **71**, 1201 (1997).

<sup>14</sup>T.-P. Hsieh, P.-C. Chiu, Y.-C. Liu, N.-T. Yeh, W.-C. Ho, and J.-I. Chyi, *J. Vac. Sci. Technol. B* **23**, 262 (2005).

<sup>15</sup>W.-H. Chang, H.-S. Chang, W.-Y. Chen, T. M. Hsu, T.-P. Hsieh, J.-I. Chyi, and N.-T. Yeh, *Phys. Rev. B* **72**, 233302 (2005).

<sup>16</sup>A. Kiraz, S. Faith, C. Becher, B. Gayral, W. V. Schoenfeld, P. M. Petroff, L. Zhang, E. Hu, and A. Imamoglu, *Phys. Rev. B* **65**, 161303(R) (2002).